https://doi.org/10.15407/ujpe63.12.1057

YU.V. KOVTUN, Y.V. SYUSKO, E.I. SKIBENKO, A.I. SKIBENKO

National Science Center Kharkiv Institute of Physics and Technology
(1, Akademichna Str., Kharkiv 61108, Ukraine; e-mail: Ykovtun@kipt.kharkov.ua)

EXPERIMENTAL STUDY OF INHOMOGENEOUS REFLEX-DISCHARGE PLASMA USING MICROWAVE REFRACTION INTERFEROMETRY

The phase shift at the plasma interferometry with oblique microwaves and microwaves passing through the center of a plasma formation has been calculated. The critical density $N_{\rm cr}$ and the critical radius $r_{\rm cr}$ of a plasma layer, at which microwaves do not hit the horn antenna, are calculated for various radial plasma distribution functions. The time dependences of the phase shift for the transverse and oblique probing modes are experimentally measured. Using the phase shifts determined by the both methods, the time dependence of the product $N_{\rm p}L$ of the electron concentration in plasma and the optical path length of a microwave beam in vacuum is found, and the average plasma density is estimated.

K e y w o r d s: plasma, plasma diagnostics, interferometry, refraction, microwave beams.

1. Introduction

Microwave methods, owing to their contactless character and the absence of temperature constraints, occupy a significant place among other methods for the plasma diagnostics [1–4]. In particular, various kinds of interferometry are widely used. Their development and application began in the mid-1950s–1960s [5–8]. In modern experimental researches in the plasma physics, microwave interferometric methods are used to measure some parameters of low-temperature weakly [9] and highly ionized [10] plasmas. They are also used to determine the parameters of a high-temperature plasma in experiments aimed at solving the problems of controlled nuclear fusion [11, 12]. Microwave plasma interferometry makes it possible to measure the average electron concentration [1–12] and the average electron collision frequency [2, 7, 8] in a plasma and to determine (to estimate) the average electron temperature [2, 8] and the electron concentration profile [2, 6–8]. In some cases, with the help of the multichord interferometry, it is possible to measure the electron concentration profile. The application of available interferometric methods requires that conditions should be created for the electromagnetic waves to pass through a plasma. Otherwise, only the value of the critical plasma density $N_{\rm cr}$ can be determined. It is worth noting that, in the course of interferometric measurements, the phase shift obtains an additional error owing to the refraction of microwave beams in a plasma [1–4, 13–16].

Methods based on the microwave refraction in an inhomogeneous plasma are also applied to the plasma diagnostics [17–22]. In particular, the oblique probing of a plasma is carried out, and either the dependence of the refraction angle on the plasma parameters [17–21] or the phase shift [22], which is used to determine the average plasma density in the corresponding cross-section segment, is determined experimentally. An important conditions for the applicability of those methods are the availability of narrow microwave beams and the validity of the geometric optics approximation. In this case, the oblique angle of

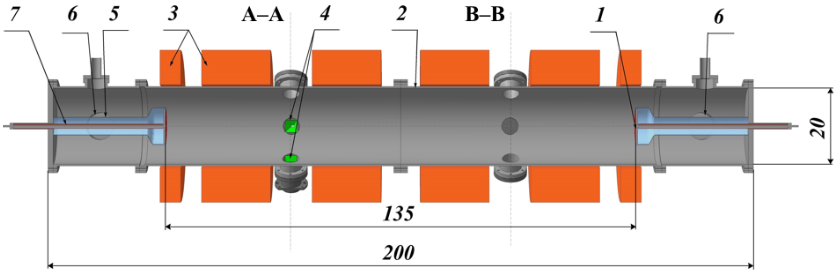

Fig. 1. Schematic diagram of the experimental MAKET installation: (*1*) cathodes, (*2*) discharge chamber (anode), (*3*) magnetic coils, (*4*) horn antennas, (*5*) and (*7*) insulators, (*6*) vacuum pumping system, A–A and B–B are cross-sections of diagnostic ports

horn antennas with respect to a plasma has to be varied in a wide interval, which is often impossible in practice. On the other hand, the beams radiated by a horn antenna diverge and, when crossing various plasma layers, can be used for the plasma diagnostics.

In works [23, 24], a possibility to use the interferometry with ordinary oblique microwaves for measuring the density in various plasma layers was studied analytically and numerically. It was shown that this method allows the plasma density to be measured in separate layers, if the density profile has a maximum that is shifted from the axis, or if the transverse probing of a plasma formation is impossible. In work [25], the deviation angle φ of a microwave beam from the angle ψ of its incidence on an inhomogeneous plasma was calculated. The results of calculations showed that some of the microwave beams could hit the horn antenna oriented at a fixed angle with respect to a plasma. The microwave scattering at fixed angles of about 60 and 120° was experimentally registered. The method of plasma interferometry with the use of oblique microwave beams, which was proposed in works [23, 24], was experimentally tested in work [26]. It was shown that the average electron concentration in the peripheral layers of a plasma can be determined when the concentration of plasma for through probing exceeds the critical value.

In works [25, 26], an inhomogeneous plasma was created in the pulsed reflex discharge. The reflex or Penning discharge is used in the physics and engineering domains dealing with the vacuum properties, atomic and electron collisions, charged particles, plasma, and so on. The plasma formed in a reflex discharge is in the crossed $\mathbf{E} \times \mathbf{B}$ fields, which leads to its drift rotation. The rotation of a plasma column in the case of multicomponent plasma gives rise to the spatial separation of the ionic component. Therefore, the reflex discharge is considered as one of the possible tools for separating the substance into mass groups [27, 28]. Modifications of a pulsed reflex discharge are also used to create low-energy high-current electron beams [29] and for the vacuum sputtering [30].

The aim of this study is to develop a method of plasma interferometry with oblique microwave beams, improve its informational content, and make the measurements more unambiguous and reliable.

2. Experimental Installation and Diagnostics

Experiments using the inhomogeneous plasma interferometry with oblique microwave beams were carried out on a MAKET installation (Fig. 1) [31]. In the installation, a powerful pulsed reflex discharge was generated in crossed $\mathbf{E} \times \mathbf{B}$ fields. The multicomponent gas-metal plasma was formed in the environment of Ar as a working gas and the sputtered cathode material. The cathodes were made of a composite material, namely, copper covered by Zr, by using the vacuum-arc deposition method. The diameter of cathodes was 10 cm. The inner side of the discharge chamber wall, which was made of a stainless steel, served as the anode. The internal diameter of a discharge chamber was 20 cm. A more detailed description of the experimental setup and plasma parameters can be found in works [10, 31–33].

The experimental conditions were as follows. The pulsed magnetic field of a seal configuration ($B \leq$ $\leq$ 0.45 T in the seal) and up to 18 ms in duration was created by a solenoid consisting of six coils (Fig. 1). The discharge voltage and current were $U \leq 4.2$ kV and $I \leq 1.8$ kA, respectively. The current

ISSN 2071-0194. Ukr. J. Phys. 2018. Vol. 63, No. 12

pulse duration was up to 1 ms. The initial pressure in the discharge chamber was 1.33×10^{-4} Pa. Then Ar was introduced, by increasing the pressure up to 0.6–3 Pa.

Figure 2 exhibits the schematic diagram of the microwave measuring system. The plasma density was measured making use of two microwave interferometers simultaneously. One of them measured the plasma density across the plasma column (Fig. 2, horn antennas *8* and *11*). The plasma density in a cross-section different from the normal one was measured by the other interferometer, whose horn antennas were disoriented by an angle of about 60° with respect to each other (Fig. 2, horn antennas *8* and *9*). Microwave radiation was emitted and received with the use of pyramidal horn antennas (Fig. 2, horn antennas *8*, *9*, and *11*) installed at diagnostic ports of cross-section A–A (Fig. 1). Their construction did not allow a possibility to change the angles of their inclination with respect to a plasma. The length and width of the cross-sections of pyramidal horns (horn aperture) were $a = b = 35$ mm. The estimation of the radiation pattern of pyramidal horns showed that the diagram half-width was about 13° in the E-plane and about 20° in the H-plane. The plasma cylinder was probed by an ordinary wave (O-wave) with the frequency $f = 37$ GHz.

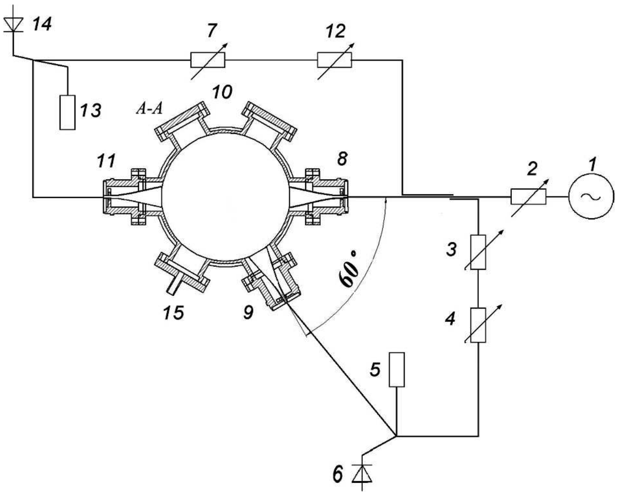

Fig. 2. Schematic diagram of the microwave measuring system: (*1*) generator; (*2*), (*3*), and (*7*) attenuators; (*4*) and (*12*) phase shifters; (*5*) and (*13*) matching loads; (*6*) and (*14*) phase detectors; (*8*), (*9*), and (*11*) horn antennas; (*10*) vacuum chamber

3. Plasma Interferometry with Oblique Microwave Beams

3.1. Phase shift at interferometric measurements

In the general case, the phase of a microwave that passed through a plasma equals

$$\Phi_{\rm p} = \frac{\omega}{c}\int\limits_0^{S_{\rm p}} n(s)ds, \qquad (1)$$

where ω is the probing frequency, c the light speed, $n(s)$ the refractive index at the point s of a plasma, and $S_{\rm p}$ is the path length of the microwave beam in a plasma, which depends on the launch angle and plasma parameters. In the case of cylindrical symmetry, Eq. (1) can be rewritten in the form [24]

$$\Phi_{\rm p} = 2\frac{\omega}{c}\int\limits_{r_0}^{R} \frac{n^2(r)rdr}{\sqrt{n^2(r)r^2 - R^2\sin^2\Psi}}, \qquad (2)$$

where R is the cylinder radius, r the current coordinate, $n(r)$ the refractive index, Ψ the angle between the beam propagation direction and the cylinder radius at the point, where the beam falls on the plasma cylinder, and r_0 is the beam trajectory turning point, which is determined from the condition

$$\frac{R^2}{{r_0}^2}\sin^2\Psi = n^2(r_0). \qquad (3)$$

At $\Psi = 0$, Eq. (2) looks like

$$\Phi_{\rm p} = 2\frac{\omega}{c}\int\limits_0^{R} n(r)dr. \qquad (4)$$

According to work [34], the refractive index for the ordinary wave in a plasma equals

$$n_0^2 = \frac{1}{2}\left(1 - \frac{{\omega_{\rm p}}^2}{\omega^2 + \upsilon_{\rm eff}^2}\right) + \\ +\frac{1}{2}\sqrt{\left(1 - \frac{{\omega_{\rm p}}^2}{\omega^2 + \upsilon_{\rm eff}^2}\right)^2 + \left(\frac{{\omega_{\rm p}}^2}{\omega^2 + \upsilon_{\rm eff}^2}\frac{\upsilon_{\rm eff}}{\omega}\right)^2}, \qquad (5)$$

where $\upsilon_{\rm eff}$ is the effective frequency of electron collisions, $\omega_{\rm p} = \left(\frac{N_{\rm p}e^2}{\epsilon_0 m_{\rm e}}\right)^{1/2}$ is the electron plasma frequency, e the elementary charge, $m_{\rm e}$ the electron

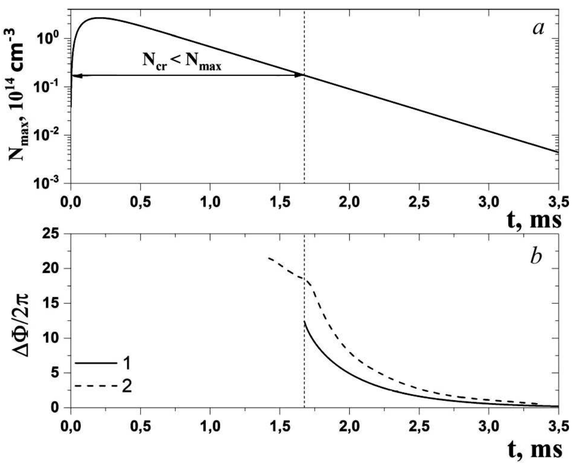

Fig. 3. Rated time dependences of the maximum plasma density (*a*) and the phase shift (*b*). The interferometry at the probing through the plasma formation center *1* and at the oblique probing *2*

mass, ϵ_0 the dielectric constant, and N_p the electron concentration in a plasma. In the case $v_\mathrm{eff}/\omega \ll 1$, expression (5) becomes much simpler,

$$n_0 = \left(1 - \frac{{\omega_\mathrm{p}}^2}{\omega^2}\right)^{1/2} = \left(1 - \frac{N_\mathrm{p}}{N_\mathrm{cr}}\right)^{1/2}, \qquad (6)$$

where $N_\mathrm{cr} = \epsilon_0 m_e \omega^2/e^2$ is the critical concentration of electrons in a plasma. In the case $\omega > \omega_p$ (i.e. $N_\mathrm{cr} > N_\mathrm{p}$), the plasma is transparent for the ordinary wave. But, at $\omega \le \omega_\mathrm{p}$ (i.e. $N_\mathrm{cr} \le N_\mathrm{p}$), it is opaque and completely reflects the microwave [34]. At the oblique incidence of a microwave on the plasma cylinder, i.e. at $\Psi \neq 0$, the wave is reflected from the plasma layer with the concentration $N = N_\mathrm{cr}\cos^2\Psi$. Furthermore, the reflected microwave acquires an additional phase shift, so that Eq. (2) reads

$$\Phi_\mathrm{p} = 2\frac{\omega}{c}\int\limits_{r_0}^{R} \frac{n^2(r)\, r\, dr}{\sqrt{n^2(r) r^2 - R^2 \sin^2\Psi}} - \frac{\pi}{2}. \qquad (7)$$

In interferometric experiments, the phase shift between two waves that passed through the reference and measurement channels is determined. This quantity equals

$$\Delta\Phi(t) = \Phi_0 - \Phi_\mathrm{p}(t), \qquad (8)$$

where $\Phi_\mathrm{p}(t)$ is the beam phase in the measurement channel, which varies, by depending on the electron concentration in a plasma [Eqs. (2)–(6)], and Φ_0 is the phase in the reference channel, which always remains constant, $\Phi_0 = (\omega/c)L$, where L is the optical path length of the microwave beam in vacuum.

After relevant transformations in Eq. (8), the average plasma density is determined by the formula

$$N_\mathrm{p}(t) = \frac{2c\Delta\Phi(t)N_\mathrm{cr}}{\omega L}. \qquad (9)$$

If the value of L is unknown, Eq. (9) is used to determine the value of the product $N_\mathrm{p}L$.

3.2. Phase shift calculation at plasma interferometry with oblique microwave beams

From the consideration carried out in Section 3 3.1, it follows that, in interferometric measurements, the phase shift depends on: the size of the region occupied by a plasma, the plasma density profile and magnitude, and the angle of incidence of a microwave on the plasma cylinder. Therefore, let us calculate the phase shift in the case where the probing beam passes through the center of a plasma formation, i.e. at the angle $\Psi = 0$, and at the oblique probing, when $\Psi \neq 0$. The initial conditions for the calculations are chosen in accordance with parameters of the experimental installation and microwave measurement system described in Section 2. In this case, the oblique probing is implemented by microwave beams emitted from the horn at the angle $\Psi \neq 0$ with respect to a plasma.

The calculations were made for a probing microwave length of 0.8 cm. In this case, the critical concentration of electrons in a plasma equals 1.7×10^{13} cm^{-3}. The plasma density profile was determined in the form [8] $N_\mathrm{p}(r) = N_\mathrm{max}F(r)$, where N_max is the electron concentration maximum at the plasma cylinder axis, and $F(r)$ the radial distribution function. In the calculations, we assumed that this function is not changed in time and selected it in the form $F(r) = 1 - (r/R)^2$, where R is the plasma cylinder radius (in this case, this parameter is equal to the radius of a vacuum chamber).

In Fig. 3, *a*, the calculated time dependence of the electron concentration maximum is shown. The phase shift was determined by formulas (2)–(4) and (6)–(8). In the case of probing through the plasma formation center, the phase shift calculations did not involve the size of a receiving horn antenna and, accordingly, the additional error induced by the refraction of microwave beams in a plasma. In the case of oblique probing, the phase shift calculations in the first approximation made allowance for the average value of the maximum and minimum phases of the beams that hit the receiving horn antenna, whose radiation reception angle, i.e. the angular coordinate of the plasma cylinder, was $\varphi = 60^\circ \pm 9^\circ$. Our previous calculations showed that if the radial distribution function has the form $F(r) = 1 - (r/R)^2$ and the maximum value of electron concentration on the axis is lower than the critical value ($N_{\rm cr} > N_{\rm max}$), the microwave beams do not hit the receiving antenna [25]. Therefore, we assumed that the microwave beams are reflected once from the opposite surface of the chamber and hit the horn antenna. The calculation results are presented in Fig. 3, *b*.

As one can see (Fig. 3, *b*, curve *1*), the interferometry through the plasma formation center demonstrates a standard picture of a decrease in the phase shift, as the plasma density decreases. At $N_{\rm cr} < N_{\rm max}$, there is no sense to talk about the phase shift, because the microwave does not pass through a plasma.

In the case of plasma interferometry with oblique microwave beams (Fig. 3, *b*, curve *2*), the phase shift is observed at $N_{\rm max} \gtrless N_{\rm cr}$. In the case $N_{\rm cr} < N_{\rm max}$, the phase shift is observed only up to a certain $N_{\rm max}$ value, because the microwave beams do not hit the receiving horn antenna at higher values. In this case, if the radius $r_{\rm cr}$ of the layer with the density equal to $N_{\rm cr}$ falls within the interval 5.2 cm $\le r_{\rm cr} \le$ 6.3 cm, then, owing to the refraction, some or all microwave beams do not hit the receiving antenna. If the critical radius is smaller than this interval, some beams turn out in a sector with the angular coordinates $\varphi = 51^\circ \div 60^\circ$; if it is larger, the beams do not hit the receiving antenna oriented at an angle $\varphi < 51^\circ$.

The calculations show that the values of $r_{\rm cr}$ for other radial distribution functions are within an interval of 4.5–6.5 cm (see Table). A comparison of phase shifts testifies that, in this case, the phase shift obtained for plasma interferometry with oblique microwave beams is larger than that for interferometry through the plasma formation center. This result can be explained as follows. In the region of the oblique beam passage, the plasma is transparent. Accordingly, one reflection from the opposite surface of the chamber was assumed in calculations. In other words, microwave beams passed through the plasma twice.

Hence, our calculations performed with rather simplified assumptions demonstrated some features and the difference between the phase shifts measured at plasma interferometry with oblique microwave beams and interferometry through the center of a plasma formation. Under real experimental conditions, the phase shift evolution in time can be more complicated.

4. Experimental Results and Their Discussion

Our previous researches of the dense gas-metal plasma created in a powerful pulsed reflex discharge [10, 31–33] showed that the time dependence of the average plasma density can be divided into three stages. The first stage includes the plasma creation and the growth of its density to the value $N_{\rm p} \approx 1.7 \times 10^{13}$ cm^{-3}. At this stage, the breakdown of the gas gap, ignition of an independent discharge with cold cathodes, formation of a weakly ionized plasma with $N_{\rm p} < 1 \times 10^{11}$ cm^{-3}, growth of the plasma density, and formation of a highly ionized plasma with a density of up to $N_{\rm p} \approx 1.7 \times 10^{13}$ cm^{-3} and a high ionization degree (≈0.98) of a scattered cathode material take place sequentially [35]. The second stage includes the existence of a highly ionized plasma with the density $N_{\rm p} > 1.7 \times 10^{13}$ cm^{-3}, when this parameter can reach a value of 10^{14} cm^{-3} and higher. At the third stage, the plasma density decreases, and the plasma decays.

Unlike our previous studies [10, 31–33], the average plasma density was measured, by using two microwave interferometers simultaneously. The corresponding oscillograms are shown in Fig. 4, *a*. In one interferometer (Fig. 2, horn antennas *8* and *11*), the probing was carried out through the center of a plasma formation (Fig. 4, *a*, oscillogram *1*). In the

The values of $r_{\rm cr}$ for other radial distribution functions

$F(r)$	$r_{\rm cr}$, cm
$[1 - (r/R)]$	5.6–6.5
$[1 - (r/R)^2]$	5.2–6.3
$[1 - (r/R)^3]$	4.3–6
$[\cos(\pi r/2R)]$	5.4–6.4
$[\cos^2(\pi r/2R)]$	5.8–6.5
$[J_0(2.405r/R)]$	5.6–6.5

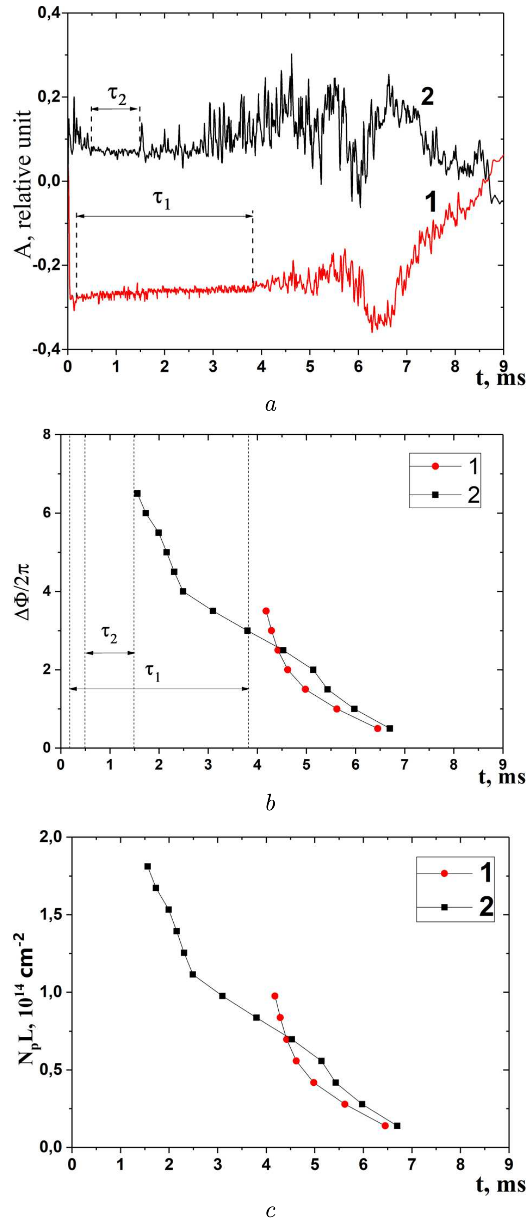

Fig. 4. Time dependences of interference signals (a), phase shift (b), and $N_\mathrm{p}L$-product (c). Interferometry with probing through the plasma formation center (*1*) and oblique probing (*2*). τ_1 and τ_2 are time intervals without phase shifts at the probing through the plasma formation center and oblique probing, respectively

other interferometer (Fig. 2, horn antennas *8* and *9*), the plasma was probed by oblique microwave beams (Fig. 4, a, oscillogram *2*). The analysis of oscillograms shows that if plasma is probed through the center of a plasma formation (Fig. 4, a, curve *1*), the standard interferometric pattern is observed. Namely, if the plasma density is lower than N_cr, the oscillogram contains the phase shifts. But if $N_\mathrm{cr} < N_\mathrm{p}$, the phase shift is absent, and the cut-off of a microwave signal takes place (the microwave does not pass through a plasma).

When probing a plasma with oblique microwave beams, the oscillogram (Fig. 4, a, curve *2*) demonstrates an interferometric picture that is similar to that described above in the case of probing through the plasma formation center, but with some essential features: the oscillogram contains phase shifts at a plasma density higher than N_cr, as well as a section with no phase shifts. The previous calculations showed (see Subsection 3.2) that the phase shift can be observed up to a certain N_max value. At higher values, microwave beams do not hit the receiver horn antenna because of their refraction in an inhomogeneous plasma. In this case, the radius r_cr of the layer with the density N_cr is within an interval from 4.5 to 6.5 cm (see Table). The measurements carried out in work [32], by using the microwave reflectometry method ($f = 37.13$ GHz), showed that this radius can reach a value of about 5 cm. In view of the uncertainty Δr_cr in the position of a reflecting layer with N_cr, which was evaluated in work [36], the radius r_cr acquires a value of about 5.25 cm. Thus, the calculation results for r_cr are in the satisfactory agreement with experimental data [32, 36]. The calculations also demonstrated the absence of a phase shift in plasma interferometry with oblique microwave beams, which is observed directly in the experiment (Fig. 4, a, curve *2*).

From oscillograms in Fig. 4, a, one can see that the time interval, when there is no phase shifts at interferometry with oblique probing, begins later, and its duration is shorter than in the case of probing through the plasma formation center. In those experiments, the average difference between the time moments, when the phase shifts disappear in both interferometers, is about 0.32 ms, and the difference between the durations of time intervals with the zero phase shift equals $\tau_1 - \tau_2 \approx 2.1$ ms. More exactly, the average time interval, when the phase shift is absent, equals $\tau_1 = 3.12 \pm 0.21$ ms at probing through the center of a plasma formation and $\tau_2 = 1.04 \pm 0.25$ ms at the oblique probing.

Figure 4, b exhibits the behavior of the phase shift change in time obtained by processing the interferograms (Fig. 4, *a*). From Fig. 4, *b*, one can see that the phase shift change is similar to the results of calculations depicted in Fig. 3, *b*, but with some substantial differences. Three intervals can be conditionally distinguished. In the first interval ($N_{\rm cr} < N_{\rm p}$), the phase shift $\Delta\Phi_1 = 0$ for the probing through the plasma formation center (Fig. 4, *b*, curve *1*) and $\Delta\Phi_2 \neq 0$ for the probing with oblique microwaves (Fig. 4, *b*, curve *2*). In the second interval (Fig. 4, *b*, a time interval of 3.8–4.6 ms), the phase shift inequality $\Delta\Phi_2 \leq \Delta\Phi_1$ is obeyed. In the third interval, the phase shift $\Delta\Phi_2$ is about one and a half times larger that the phase shift $\Delta\Phi_1$. In this interval, microwave beams can be reflected from the surface of the opposite chamber wall and hit the receiving horn antenna.

The discrepancy between the phase shift behavior calculated numerically (Fig. 3, *b*) and measured experimentally (Fig. 4, *b*) is a result of several factors. First, the model function of the radial plasma density distribution that was chosen for calculations can differ significantly from the actual experimental one. Moreover, this function can change in time in the experiment, which was not taken into account in the calculations. Second, the plasma parameters always fluctuate, which results in the microwave screening in a plasma [2, 4, 37, 38], especially in a turbulent one.

Unlike the probing through the plasma formation center, the trajectory of a microwave beam in a plasma and, as a result, the L-value can change significantly at the oblique probing. Therefore, in order to analyze the time dependence of the plasma density, let us consider this parameter in the form of the product $N_{\rm p}L$ (Fig. 4, *c*). One can see that, at $N_{\rm cr} < N_{\rm p}$ ($t \leq 3.8$ ms), the oblique plasma probing (Fig. 4, *c*, curve *1*) gives a value of the plasma density corresponding to the peripheral plasma region, when the determination of the average plasma density by the probing through the center of a plasma formation is impossible. At lower plasma densities, $N_{\rm cr} > N_{\rm p}$ ($t > 3.8$ ms), the measured value of $N_{\rm p}L$ is larger for the oblique probing (Fig. 4, *c*, curve *1*), than for the probing through the plasma center (Fig. 4, *c*, curve *2*). This difference can be a result of the difference between the L-values obtained at the normal and oblique plasma probings.

To estimate the average plasma density, let us assume that the quantity $L = L_1$ does not change in time and equals $L_1 = 20$ cm for the probing through the center of a plasma. In the case of oblique probing, the quantity $L = L_2$ can change permanently in time due to the variations in both the radial distribution function and the plasma density. However, for the estimation, we assume that the L_2-value is constant within two time intervals: (i) at $t \leq 3.8$ ms ($N_{\rm cr} < N_{\rm p}$), let $L_2 \approx 10$ cm, i.e. $2L_2 \approx L_1$, and (ii) at $t > 3.8$ ms ($N_{\rm cr} > N_{\rm p}$), let $L_2 \approx 30$ cm, i.e. $L_2 \approx 1.5L_1$. The results of calculations are presented in Fig. 5. As one can see from this figure, if the plasma density $N_{\rm cr} > N_{\rm max}$, the estimates give close values of the average plasma density in both cases (oblique probing and probing through the plasma center). Those values are in satisfactory consistency with the assumption about the reflection of microwave beams from the opposite surface (i.e. the microwave beams pass through a plasma twice). In the case $N_{\rm cr} < N_{\rm max}$, the oblique probing immediately allows one to estimate the average plasma density in the peripheral layers (Fig. 5, curve *2*).

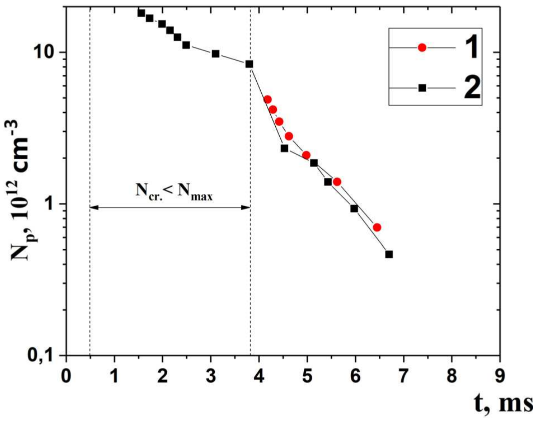

Fig. 5. Time dependences of the average plasma density. Interferometry with the probing through the plasma formation center (*1*) and oblique probing (*2*)

5. Conclusions

1. The calculations of the phase shifts at the probing through the plasma formation center and at the oblique probing showed that, in the latter case, the phase shift is observed both at $N_{\rm cr} > N_{\rm max}$ and at $N_{\rm cr} < N_{\rm max}$. In the case $N_{\rm cr} < N_{\rm max}$, the phase shift takes place to a certain N_{max}-value, when the microwave beams do not hit the receiving horn antenna. The calculations of the critical radius $r_{\rm cr}$ of the plasma layer with the density $N_{\rm cr}$, when the beams do not hit the antenna, showed that the value of $r_{\rm cr}$

falls within the interval from 4.5 to 6.5 cm for various radial distribution functions of the plasma density.

2. The experimental results showed that three intervals can be conditionally distinguished in the time dependence of the phase shift change. In the first interval at $N_{\rm cr} < N_{\rm p}$, there is no phase shift $\Delta\Phi_1$ for the probing through the plasma formation center, and there is the phase shift $\Delta\Phi_2$ for the probing of a plasma with oblique microwaves. In the second interval, the phase shifts are $\Delta\Phi_2 \leq \Delta\Phi_1$. In the third interval, the phase shift $\Delta\Phi_2$ is about one and a half times larger that the phase shift $\Delta\Phi_1$.

3. The experimentally measured average time interval, when there is no phase shifts, equals $\tau_1 = 3.12 \pm 0.21$ ms at the probing through the plasma formation center, and $\tau_2 = 1.04 \pm 0.25$ at the oblique probing.

4. The time dependence of the product $N_{\rm p}L$ was determined, and the average plasma density at the oblique probing and the probing through the plasma center was estimated. In both cases, close values of the plasma density were obtained at $N_{\rm cr} > N_{\rm p}$, which are in satisfactory agreement with the assumption about the microwave radiation reflection from the opposite chamber surface. In the case $N_{\rm cr} < N_{\rm p}$, the oblique probing makes it possible to directly estimate the average plasma density in peripheral layers.

1. M.A. Heald, C.B. Wharton. *Plasma Diagnostics with Microwaves* (Wiley, 1965).
2. V.E. Golant. *Superhigh-Frequency Methods of Plasma Research* (Nauka, 1968) (in Russian).
3. H.-J. Hartfuss, T. Geist. *Fusion Plasma Diagnostics with mm-Waves: An Introduction* (Wiley-VCH, 2013) [ISBN: 978-3-527-41105-4].
4. E. Mazzucato. *Electromagnetic Waves for Thermonuclear Fusion Research* (World Scientific, 2014) [ISBN: 978-981-4571-80-7].
5. R.F. Whitmer. Microwave studies of the electron loss processes in gaseous discharges. *Phys. Rev.* **104**, 572 (1956).
6. C.B. Wharton, D.M. Slager. Microwave determination of plasma density profiles. *J. Appl. Phys.* **31**, 428 (1960).
7. L.O. Dushyn, V.I. Kononenko, R.I. Kovtun, A.I. Skibenko, K.D. Sinelnikov, V.T. Tolok. Plasma study using a microwave interferometer. *Ukr. Fiz. Zh.* 8, 740 (1963) (in Ukrainian).
8. L.O. Dushyn, V.I. Kononenko, R.I. Kovtun, V.I. Pryvezentsev, A.I. Skibenko. The use of interferometer and microwave cut-off method for plasma research. *Ukr. Fiz. Zh.* **10**, 977 (1965).
9. K. Dittmann, C. Kullig, J. Meichsner. 160-GHz Gaussian beam microwave interferometry in low-density RF plasmas. *Plasma Sourc. Sci. Technol.* **21**, 024001 (2012).
10. Yu.V. Kovtun, A.I. Skibenko, E.I. Skibenko, Yu.V. Larin, A.N. Shapoval, E.D. Volkov, V.B. Yuferov. Study of multicomponent plasma parameters in the pulsed reflex discharge. *Ukr. J. Phys.* **55**, 1269 (2010).
11. R.O. Pavlichenko, N.V. Zamanov, A.E. Kulaga. First measurements of line electron density in Uragan-2M plasmas via 140 GHz heterodyne interferometer. *Probl. At. Sci. Tech.* No. 1, 257 (2017).
12. M. Varavin, J. Zajac, F. Zacek, S. Nanobashvili, G.P. Ermak, A.V. Varavin, A.S. Vasilev, M. Stumbora, A. Vetoshko, A.V. Fateev, V.V. Shevchenko. New design of microwave interferometer for tokamak compass. *Telecommun. Radio Eng.* **73**, 935 (2014).
13. I.E. Arsaev, B.E. Kinber, N.N. Ivanchinov-Marinskii. Influence of the medium refraction and absorption on the transmission coefficient between two antennas at plasma diagnostics. *Zh. Tekhn. Fiz.* **37**, 1495 (1967) (in Russian).
14. V.G. Grigorenko, L.A. Dushin, A.I. Skibenko. Influence of refraction on the determination accuracy of plasma density in microwave interferometry. In *High-Frequency Plasma Properties* (Naukova Dumka, 1968), p. 178 (in Russian).
15. B. Anichin, Influence of refraction on radio interferometric measurements of electron density distribution. *Zh. Tekhn. Fiz.* **39**, 478 (1969) (in Russian).
16. V.G. Petrov, Influence of refraction on plasma density measurements. *Plasma Phys. Rep.* **32**, 311 (2006).
17. M.M.Z. Kharadly, A new millimetre-wave method for determination of electron-density profiles in a linear discharge. *Proc. IEE* **110**, 1202 (1963).
18. B.A. Anicin. Electron density profiles in cylindrical plasmas from microwave refraction data. *Radio Sci. J. Res.* **69D**, 721 (1965).
19. L.A. Dushin, V.I. Kononenko, V.L. Sizonenko. A.I. Skibenko, K.N. Stepanov. Determination of the spatial distribution of plasma density by microwave beam refraction. *Zh. Tekhn. Fiz.* **36**, 304 (1966) (in Russian).
20. L.A. Dushin, V.I. Kononenko, A.I. Skibenko. Determination of the spatial distribution of plasma density by refraction of microwave beams with several frequency components. *Zh. Tekhn. Fiz.* **36**, 1842 (1966) (in Russian).
21. V.V. Nemov, V.L. Sizonenko, K.N. Stepanov, J. Teichman, Methods of determining the density and temperature distribution of a plasma using electromagnetic waves. *Nucl. Fusion* **9**, 243 (1969).
22. A.R. Jones, B.V. Stanic, E.R. Wooding. Plasma-density determination from the phase shift in scattered radiation. *Electron. Lett.* **4**, 392 (1968).
23. A.I Skibenko, I.B. Pinos, Yu.V. Kovtun, E.I. Skibenko. Plasma interferometry using refraction of oblique microwave beams. In *Abstracts of the Ukrainian Conference on Plasma Physics and Controlled Thermonuclear Fusion, September 22–23, 2015, Kyiv* (2015), p. 55 (in Ukrainian).
24. A.I. Skibenko, I.B. Pinos, Yu.V. Kovtun, E.I. Skibenko, E.V. Syus'ko, Application of microwave beam refraction in

inhomogeneous plasma interferometry. *Ukr. J. Phys.* **61**, 715 (2016).
25. Yu.V. Kovtun, E.V. Syus'ko, E.I. Skibenko, A.I. Skibenko, Refraction of microwaves in an inhomogeneous rotating plasma. *Probl. At. Sci. Tech.* No. 6, 169 (2016).
26. Yu.V. Kovtun, E.I. Skibenko, A.I. Skibenko, A.N. Ozerov, I.B. Pinos, E.V. Syus'ko. Interferometry of plasma with the use of the microwave ray refraction. In: *2016 9th International Kharkiv Symposium on Physics and Engineering of Microwaves, Millimeter and Submillimeter Waves (MSMW)* (Kharkiv, 2016), p. 1–4.
27. E.I. Skibenko, Yu.V. Kovtun, A.M. Egorov,V.B. Yuferov. Material separation into elements based on the physical principles of beam-plasma and reflex discharges. *Probl. At. Sci. Tech.* No. 2, 141 (2011).
28. D.A. Dolgolenko, Y.A. Muromkin. Separation of mixtures of chemical elements in plasma. *Physics-Uspekhi* **60**, 994 (2017).
29. G.E. Ozur, D.I. Proskurovsky. Generation of low-energy high-current electron beams in plasma-anode electron guns. *Plasma Phys. Rep.* **44**, 18 (2018).
30. T. Kimura, R. Yoshida, T. Mishima, K. Azuma, S. Naka. Preparation of TiN films by reactive high-power pulsed sputtering Penning discharges. *Jpn. J. Appl. Phys.* **57**, 06JE02 (2018).
31. Yu.V. Kovtun. Features of dense plasma formation in the reflex discharge on gas-metal mixes. *Probl. At. Sci. Tech.* No. 4, 38 (2013).
32. Yu.V. Kovtun, E.I. Skibenko, A.I. Skibenko, V.B. Yuferov. Rotation of plasma layers with various densities in crossed $E \times B$ fields. *Ukr. J. Phys.* **58**, 450 (2013).
33. Yu.V. Kovtun, A.I. Skibenko, E.I. Skibenko, Yu.V. Larin, A.N. Shapoval, E.D. Volkov, V.B. Yuferov. Study of the parameters of hydrogen-titanium plasma in a pulsed reflective discharge. *Plasma Phys. Rep.* **36**, 1065 (2010).
34. V.L. Ginzburg. *Propagation of Electromagnetic Waves in Plasma* (Gordon and Breach, 1961).
35. Yu.V. Kovtun, E.I. Skibenko, A.I. Skibenko, V.B. Yuferov. Estimation of the efficiency of material injection into the reflex discharge by sputtering the cathode material. *Ukr. J. Phys.* **57**, 901 (2012).
36. Yu.V. Kovtun, A.I. Skibenko, E.I. Skibenko, V.B. Yuferov. Analysis of errors in the plasma rotation velocity measurement by the method of microwave correlation reflectometry. In: *2013 International Kharkov Symposium on Physics and Engineering of Microwaves, Millimeter and Submillimeter Waves* (Kharkiv, 2013), p. 554.
37. L.A. Dushin, A.I. Skibenko, I.P. Fomin, V.A. Pimkin, V.V. Zinoviev. Angular dispersion of microwave flux in fluctuating plasma. In *Plasma Physics and Problems of Controlled Thermonucler Synthesis* (Naukova Dumka, 1971), Vol. 1, p. 52 (in Russian).
38. E. Gusakov, M. Irzak, A. Popov, Radial correlation reflectometry at oblique probing wave incidence (Linear scattering theory predictions). *Plasma Phys. Control. Fus.* **56**, 025009 (2014).

Received 09.01.18.
Translated from Ukrainian by O.I. Voitenko

Ю.В. Ковтун, Є.В. Сюсько,
Є.І. Скібенко, А.І. Скибенко

ЕКСПЕРИМЕНТАЛЬНЕ ДОСЛІДЖЕННЯ НЕОДНОРІДНОЇ ПЛАЗМИ ВІДБИВНОГО РОЗРЯДУ ЗА ДОПОМОГОЮ ІНТЕРФЕРОМЕТРА НА ОСНОВІ РЕФРАКЦІЇ МІКРОХВИЛЬ

Р е з ю м е

Проведено розрахунок фазового зсуву при інтерферометрії плазми похилими мікрохвилями та крізь центр плазмового утворення. Розраховано значення критичного радіуса $r_{\rm cr}$ плазмового шару з густиною рівній $N_{\rm cr}$, для різноманітних функцій розподілу вздовж радіуса, коли мікрохвильові промені не потрапляють до антени. Експериментально отримана часова залежність зміни фазового зсуву для наскрізного та похилого зондування. З фазових зсувів, виміряних обома інтерферометрами, визначено залежність добутку $N_{\rm p}L$ ($N_{\rm p}$ – концентрація електронів плазми, L – довжина оптичного шляху мікрохвильового променя в вакуумі) у часі, а також оцінено величину середньої густини плазми.